Journal of Crystal Growth 474 (2017) 81–88

Contents lists available at ScienceDirect

Journal of Crystal Growth

journal homepage: www.elsevier.com/locate/jcrysgro

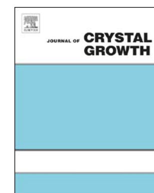

3D numerical analysis of influence of the non-uniform deposition rate on the hillock density at HVPE-GaN surface

Xue-Feng Han[a], Jae-Hak Lee[b], Yoo-Jin Lee[b], Jae-Ho Song[b], Kyung-Woo Yi[a,*]

[a] Department of Materials Science and Engineering, Seoul National University, Seoul 151-744, Republic of Korea
[b] TGO Tech, Hwasung-City, Gyeonggi-Do, 445-812, Republic of Korea

ARTICLE INFO

Communicated by Dr Francois Dupret

Keywords:
A1.Computer simulation
A1.Fluid flows
A3.Hydride vapor phase epitaxy
B1.GaN

ABSTRACT

In this study, hydride vapor phase epitaxy (HVPE), one of the feasible methods to produce the GaN thin film, has been used to conduct experiments under different temperatures. In order to study the factors affecting the distribution of the density of the hillocks along radial direction, we have conducted a 3D calculation to observe the fluid flow, mass transfer and deposition rate distribution using the CFD-ACE program. The numerical results have shown that the wafers have experienced high and low growth rate alternately. The growth rate fluctuations at different distances from the inlets are compared by standard deviation analysis. These standard deviations of deposition rates along the azimuthal direction increase from the center to the periphery, which might explain why the density of the hillocks increases from the center to the periphery in the experiments. Moreover, it is found that the non-uniform deposition rates are the result of low speed rotation of the susceptor. Increasing the rotation speed of the susceptor increases the uniformity of the gas flow pattern and deposition rate, which means that the high rotation speed can decrease the standard deviation of the deposition rate along azimuthal direction. Consequently, the density of the hillocks can be decreased.

1. Introduction

During the few past decades, GaN thin film growth technology has tremendously developed because of its wide band gap well applicable to laser diodes (LDs) and light emitting diodes (LEDs) [1,2]. Until now, due to the limitation of the feasible methods to grow bulk GaN with large dimension and high purity, epitaxy is the most popular method to fabricate GaN thin films. Among the epitaxy methods, hydride vapor phase epitaxy (HVPE) is widely employed to produce GaN templates for the LED chips [3]. Considering that the cost effectiveness of LED light bulb is the key factor to replace the traditional lamp, hence improving the efficiency of energy consumption, HVPE equipment capable of producing high quality GaN on large sapphire wafers with high throughput is urgently required to improve the competitiveness of LED application [4].

However, when the number or the size of the wafers is increased, not only the non-uniformity of the deposition thickness becomes severer [5,6] but also the surface morphology becomes more difficult to control [7]. Surface morphology is extremely important since a rough interface will result in poor device performance [8]. Among the surface defects frequently occurring with III-V semiconductors, hillocks have been investigated in many previous studies [8–14]. A.R.A Zauner asserted that the misorientation of substrate caused the hillock formation by comparing the surface morphology of GaN grown on different oriented GaN substrates [9]. Moreover, according to T. B. Wei [10], the radius of the spiral is huge due to a high growth rate and a large strain. F. Oehler also have meticulously observed the hillocks, concluding that the formation of hillocks is linked to screw dislocations [11]. Through cathodoluminescence (CL) and atomic force microscopy (AFM) measurements, K. Zhou believes that a larger strain field around a dislocation cluster rather than a single dislocation may be the reason for hillock formation [8]. Pawel Kempisty asserts that the non-uniformity of the growth rate may also lead to significant strains in GaN material [15].

In this study, hillocks have been observed at the surface of GaN thin film grown by HVPE. It is found that the density of the hillocks increases along the radial direction from the center to the periphery. In order to explore the factor resulting in a high density of screw dislocations, a steady 3D numerical simulation has been conducted. The calculation results and experimental results show an explicit correlation between the density of hillocks and the deposition rate change, which provides support for the idea that non-uniformity of the growth rate may also lead to significant strain. Moreover, through a comparison of the deviations of the deposition rate between different

* Corresponding author.
E-mail address: yikw@snu.ac.kr (K.-W. Yi).

http://dx.doi.org/10.1016/j.jcrysgro.2016.12.081

Available online 22 December 2016
0022-0248/ © 2016 Elsevier B.V. All rights reserved.

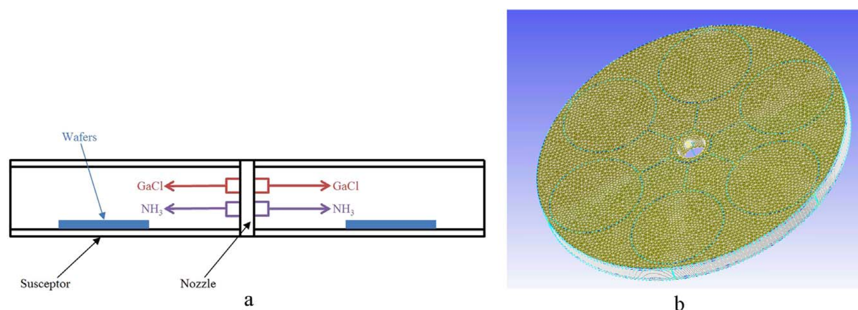

Fig. 1. (a) Schematic diagram of the vertical cross section of HVPE equipment. (b) 3D Numerical model of the HVPE equipment.

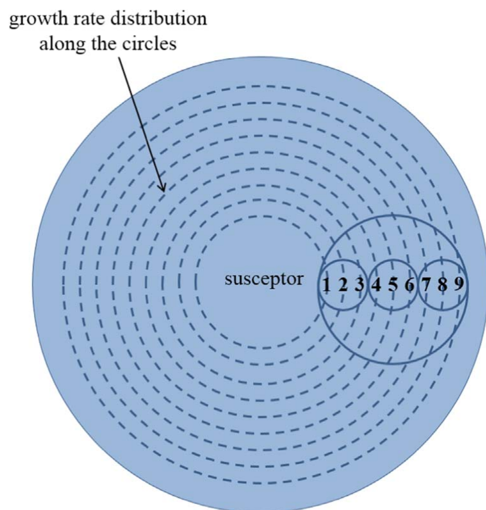

Fig. 2. Schematic diagram of the positions of wafers and nine probe curves along the azimuthal direction (curve 1–3 are for wafer P2, curve 4–6 are for wafer P4, curve 7–9 are for wafer P6).

rotation speeds, it is predicted that high rotation speed will decrease the density of the hillocks.

2. Experimental procedure

2.1. Experiments

In the present study, a multi-wafer horizontal HVPE reactor has been designed. The schematic diagram of the reactor is shown in Fig. 1a. Six 6-in. wafer slots have been designed to make it capable of depositing 6 sapphire wafers in a single run. Reacting gases and carrier gas are fed from the center of the reactor and flow away through the peripheral gap between the susceptor and furnace wall. To increase the uniformity of the deposition thickness between different wafers, the susceptor is rotating at a constant speed. The susceptor is made up of quartz to withstand the high temperature. The experiments of growing GaN thin film on sapphire wafers have been conducted at 1193 K and 1223 K. The pressure in the equipment is 1 bar. In order to decrease the cost of the experiments, 6 in. wafers are replaced by three 2-in. wafers arranged in a row as shown in Fig. 2. The growth time is 30 min. After the deposition, the surface morphology of GaN thin film is

Table 2
Major conditions in the calculations.

Temperature	Pressure	Susceptor Rotation speed	Inlet	Outlet	Wall
1193 K/1223 K	1 bar	5 RPM	Constant volume per minute	Constant pressure	Adiabatic

observed through the OLS4000 3D laser measuring microscope.

2.2. Calculations

A 3-D simulation model consistent with the HVPE equipment has been constructed with unstructured cells as shown in Fig. 1b. Due to the longtime growth process and steady flow of reacting gases, the calculations of the model have been conducted in steady state, which is beneficial to the computational efficiency. Mass transfer and surface reaction have been implemented to calculate the mass fraction of the gases and deposition rate. Heat transfer is not necessary because, differently from the temperature distribution obtained when only susceptor is heated by induction, the simulation domain has a very uniform temperature distribution as the entire heat zone is heated by the resistance heating elements. According to the measurement by thermocouples in the experiment, the deviation of the temperature is less than 1 K.

The mass transfer equations are as follows:

$$\rho\frac{Dv}{Dt}=\eta\nabla^2 v-\nabla P+\rho g \quad (1)$$

$$\rho\frac{\partial\rho}{\partial t}+\nabla\bullet(\rho\vec{v})=0 \quad (2)$$

In these equations, P, η, t, ρ, g and v are the pressure (Pa), viscosity (kg/m/s), time (s), density (kg/m^3), gravity (m/s^2) and velocity vector (m/s). Surface reaction has been modeled on the susceptor in our simulation. So the primary chemical equation to deposit GaN thin film is as follows [16–18]:

$$GaCl+NH_3=GaN(Bulk)+HCl+H_2 \quad (3)$$

It is known that ammonia is decomposed at high temperature. The decomposition of NH_3 also has been considered in the surface

Table 1
Physical properties of gases and susceptor employed in the calculations.

	Density	Heat capacity	Thermal conductivity	Viscosity	Mass diffusivity
Gases	Ideal gas law	Mix JANNAF method	Mix kinetic theory	Mix kinetic theory	Schmidt number 0.7
Susceptor	2200 kg/m^3	670 J/(kg·K)	1.4 W/(m·K)	–	–

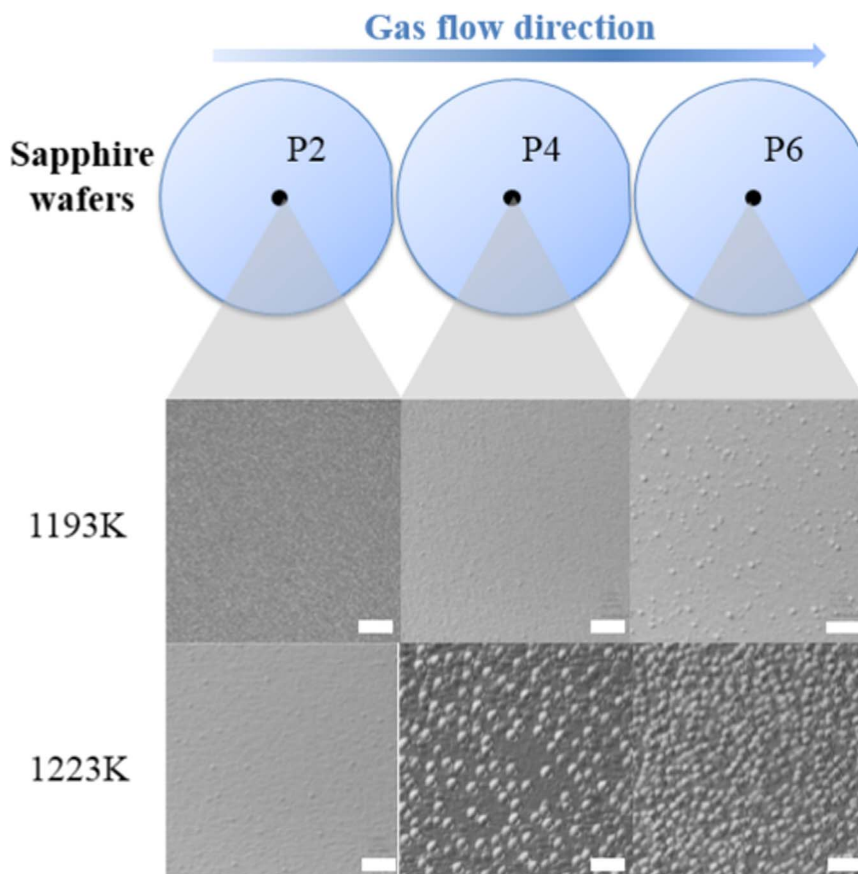

Fig. 3. Surface morphology taken from the center of the P2, P4 and P6 sapphire wafers by 3D laser measuring microscope (white scale bar is 320 μm).

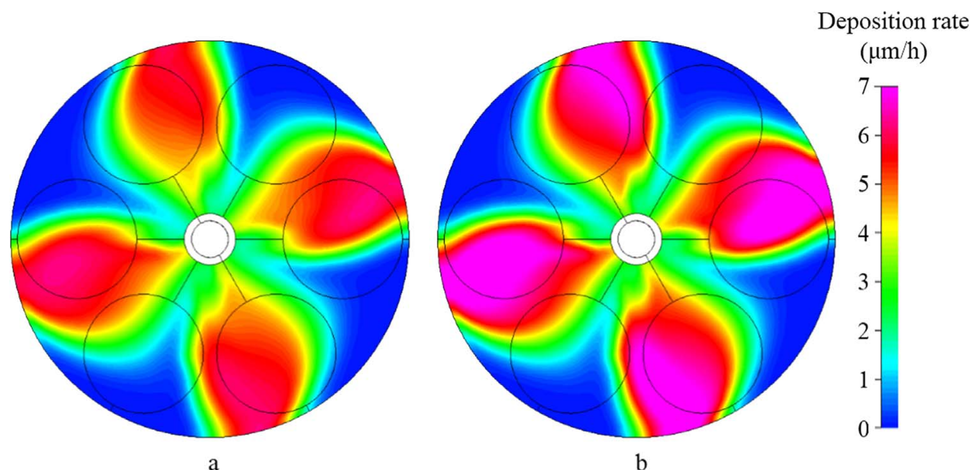

Fig. 4. Deposition rate distributions at different temperatures: (a) 1193 K; (b) 1223 K.

reactions.

$$2NH_3=N_2+3H_2 \quad (4)$$

To ensure the completeness of the reaction of GaCl, the quantity of ammonia is excessive in the experiment. The deposition rate of GaN mainly depends on the transportation fluxes of GaCl molecules from gas phase to the surface. The driving force and the direction of GaCl transportation are decided by the partial pressure of the GaCl gas. The following equations describe the relation between the partial pressures and the transportations of the gases considered in the simulation:

$$J_i=\alpha_i\beta_i(P_i^w-P_i^e) \quad (5)$$

$$\beta_i=(2\pi\mu_i RT)^{-1/2} \quad (6)$$

Here, J_i is the molar flux (kg/(m^{2}s)), T is temperature (K), μ_i is the molar mass (g/mol), R is the gas constant, P_i^w is the partial pressure (Pa) at the surface, P_i^e is the equilibrium pressure (Pa), as calculated from the standard free energy change of reaction (3) and the partial pressures of the other gas components, and α_i is the sticking coefficient.

Table 1 shows the physical properties of the gases and susceptor. The specific property of each gas involved in the calculation refers to the CFD-ACE database. The properties of the mixture of gases are calculated from each gas species by the models of Table 1. The gases are regarded as compressible fluids so that the ideal gas law is

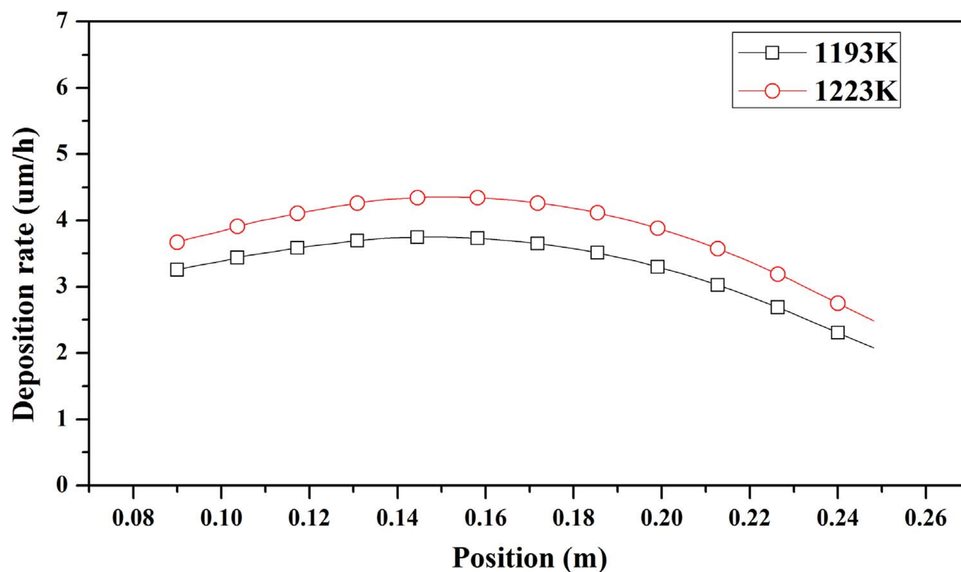

Fig. 5. Deposition rate distributions along the radial direction at 1193 K and 1223 K.

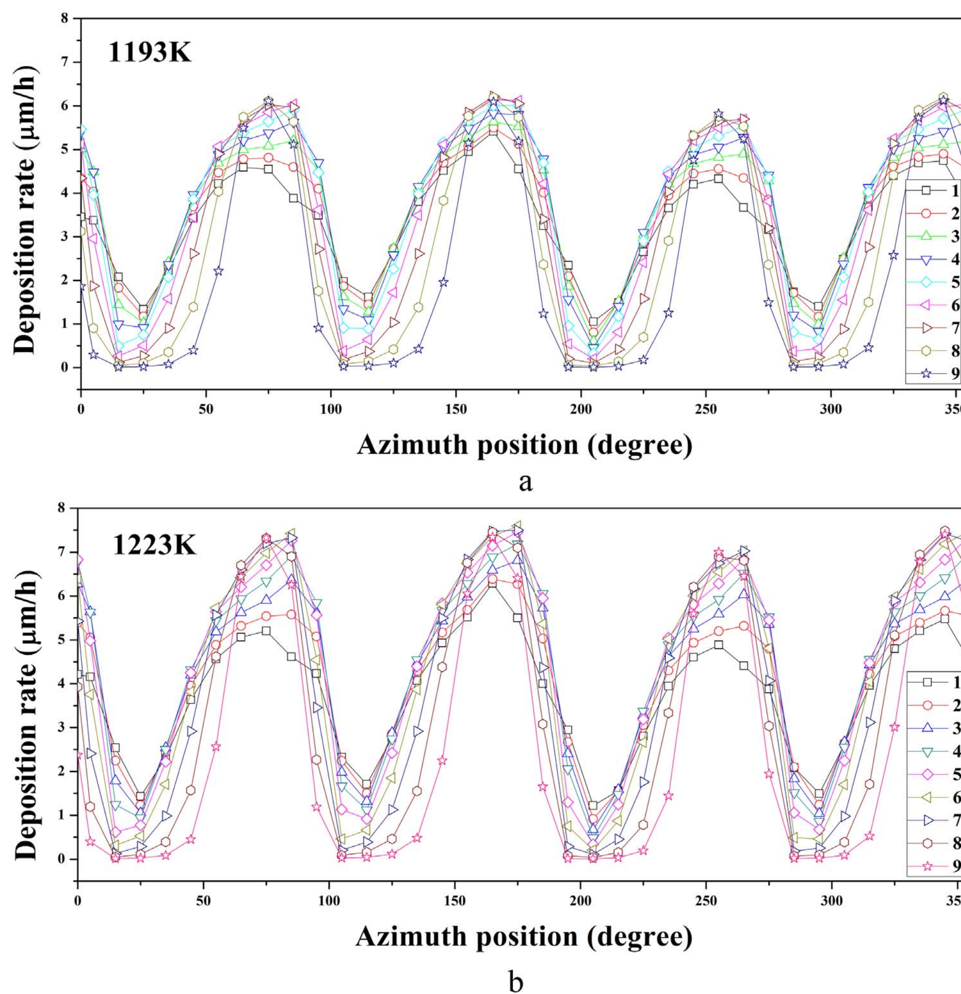

Fig. 6. Deposition rate distributions along azimuthal direction at different temperatures: (a) 1193 K; (b) 1223 K.

employed. The susceptor is made up of quartz, the properties of which are also shown in Table 1.

To be compared with the experimental results, calculations have been conducted at 1193 K and 1223 K. As shown in Table 2, the pressure is at a constant value of 1 bar. The susceptor is rotating at 5 RPM. The gases are fed from the inlets at the center with a constant volume per minute at a constant pressure. The outer wall of the model is designated as adiabatic wall. The gravity is 9.8 m/s^2.

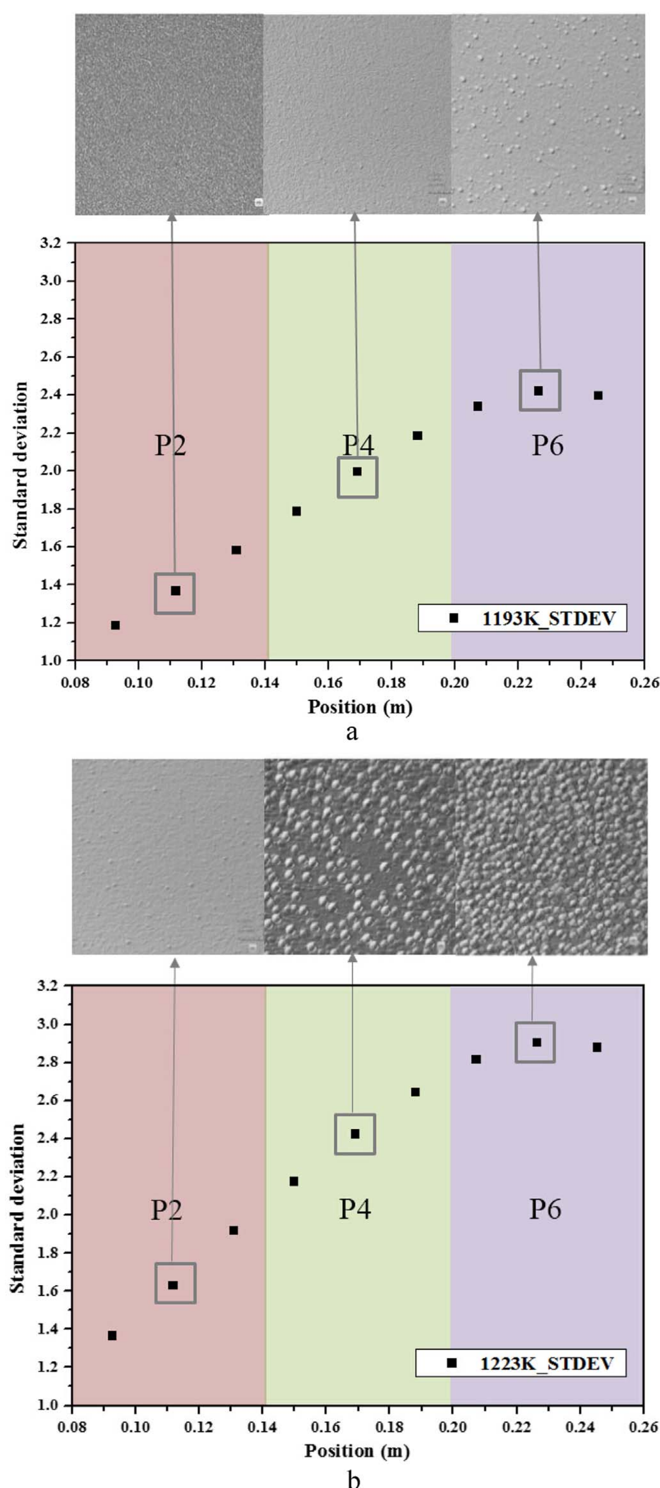

Fig. 7. Comparison between the hillock distribution and the deviation of the deposition rate along the radial direction for P2, P4 and P6 wafers at: (a) 1193 K; (b) 1223 K.

3. Results and discussion

3.1. Hillock distribution at the GaN surface

Hillocks have been observed from the experiments at both 1193 K and 1223 K. Fig. 3 shows the surface morphology obtained from the center of the P2, P4 and P6 sapphire wafers (the three 2-in. wafers are called P2, P4 and P6 from center to periphery.) by 3D laser measuring microscope. The hillocks at 1223 K are larger than the hillocks at 1193 K. Moreover, from the comparison between the three wafers, it is clearly seen that the density of the hillocks increases from P2 to P6.

To exactly illustrate the increase of the hillocks, the quantity of hillocks is calculated by the image processing application of the MATLAB code. Because the dimensions of the hillocks at 1193 K and 1223 K are different, the identified critical sizes for these two temperatures are defined differently to make the densities of the hillocks of P2 wafers as zero at both 1193 K and 1223 K. At 1193 K, from P2 to P6, the densities of the hillocks are 0 cm^{-2}, 1.83×10^2 cm^{-2}, 1.51×10^3 cm^{-2}; at 1223 K, from P2 to P6, the densities of the hillocks investigated are 0 cm^{-2}, 5.79×10^2 cm^{-2}, 2.70×10^3 cm^{-2}.

3.2. Growth rate distribution along the radial direction

Through the numerical calculations, the growth rate distributions at the susceptor and wafer have been obtained under the temperatures of 1193 K and 1223 K, as shown in Fig. 4. The patterns of the deposition rate distributions are both 4-fold due to the four-way flow design of the gas inlets. The deposition rate at 1223 K is larger than that at 1193 K because the sticking coefficient is higher at a higher temperature. After averaging the deposition rates along the azimuthal direction and plotting them along the radial direction, the comparison of the deposition rate distributions along the radial direction between 1193 K and 1223 K is shown in Fig. 5. The trends of the deposition rate under 1193 K and 1223 K are similar so that both curves increase at the upstream extremity and decrease at the downstream extremity, which is identical to our previous research results [6].

In both cases, the positions of maximum growth rate and maximum hillock density are different. Also the hillock density of P2 at 1223 K is smaller than that of P4 and P6 at1193 K. Even the growth rate of P2 at 1223 K is faster than that of P4 and P6 at 1193 K. Therefore, we could conclude that the density of hillocks is not increased by increasing the deposition rate.

3.3. Growth rate distribution along azimuthal direction

Since the susceptor keeps rotating during the operation, a certain position on the sapphire wafers will experience high and low growth rate, alternately four times for each rotation. Therefore, the degree of deposition rate change has been investigated by comparing the deposition rate distributions along the azimuthal direction at different radii. As shown in Fig. 2, nine curve probe curves have been selected from the nearest point of P2 to the farthest point of P6 from the inlets. Curves 1, 2 and 3 are associated with the nearest point, center point and farthest point of P2. In the same way, there are in total nine probe curves employed to plot the deposition rates. Fig. 6 shows the deposition rate distribution along the azimuthal direction at 1193 K and 1223 K. The black squares in both Fig. 6a and b, which indicate the nearest point of P2, obviously have the smallest fluctuation. From curve 1 to curve 8, the fluctuation becomes gradually large.

To evaluate and compare the degree of fluctuation of the deposition rate between the probe curves with different radii, the standard deviation of the deposition rate along the rotation direction has been introduced. Fig. 7 shows a comparison between the hillocks and standard deviation of the deposition rate along the rotation direction at 1193 K and 1223 K. The density of hillocks at 1223 K is larger than that at 1193 K and this seems to support the idea that high deposition rates increase the hillock density. However, through a comparison between Figs. 7a and b, it is seen that the standard deviations at 1223 K are larger than those at 1193 K, which is the reason why the density of hillocks at 1223 K is larger than that at 1193 K. Besides, the deviation distribution shows a same trend at 1193 K and 1223 K, indicating that along the flow direction, the deviation increases gradually and decreases slightly at the end of P6. Accordingly, the density of the hillocks increases from the center of P2 to the center of P6. So the present study strongly supports the idea that non-uniform deposition rate could induce hillocks [15].

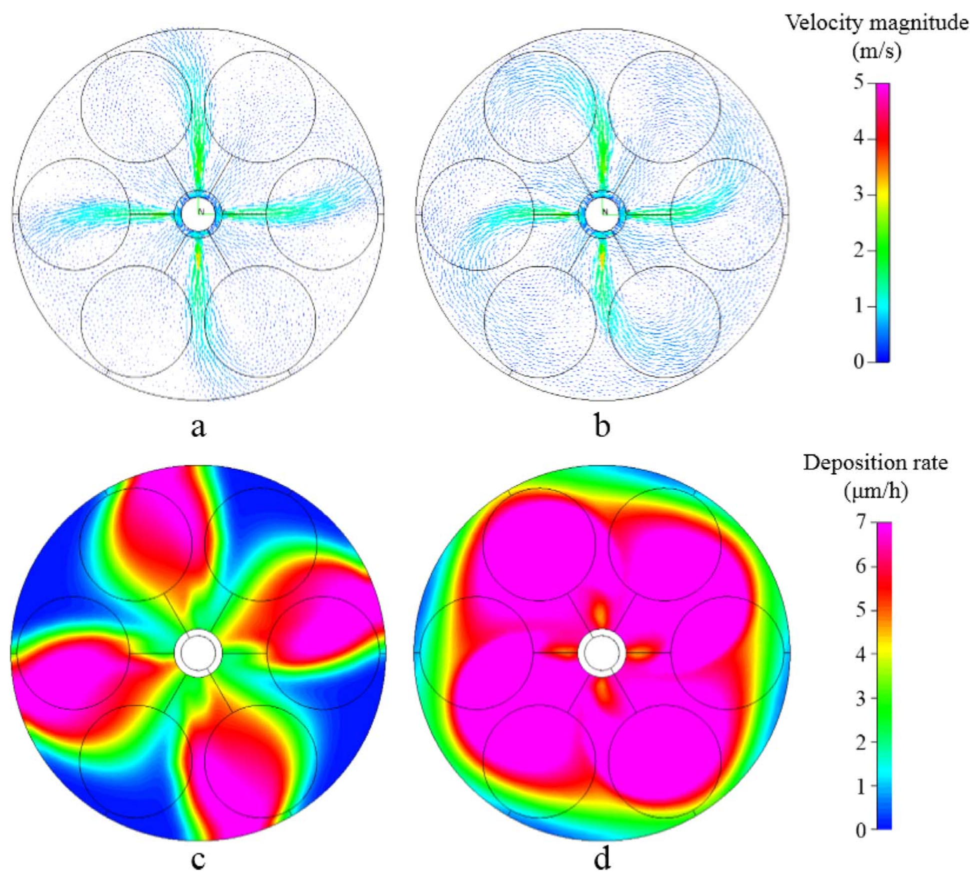

Fig. 8. Flow velocity vector and deposition rate distributions at 1223 K under different rotation speeds: (a) flow velocity vector distribution at the horizontal symmetry plane under 5 RPM; (b) flow velocity vector distribution on the horizontal symmetry plane under 15 RPM; (c) deposition rate distribution under 5 RPM; (d) deposition rate distribution under 15 RPM. (For interpretation of the references to color in this figure, the reader is referred to the web version of this article.)

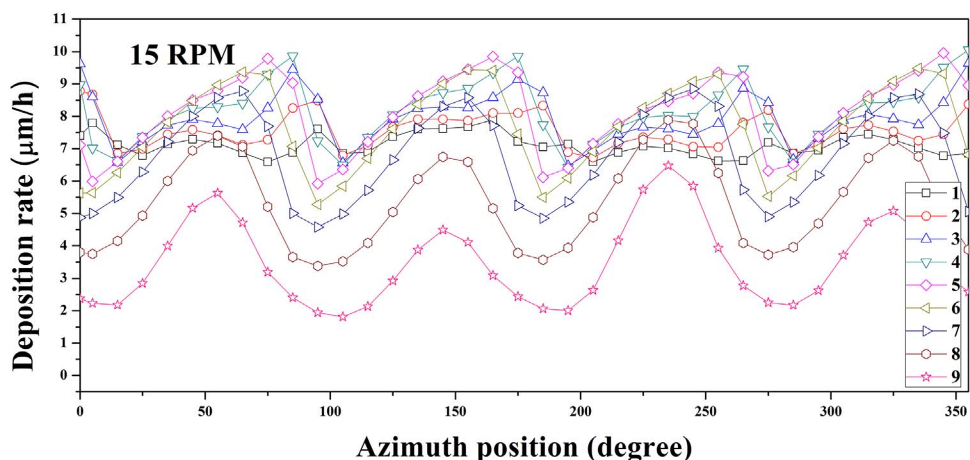

Fig. 9. Deposition rate distribution along azimuthal direction at rotation speed of 15 RPM.

3.4. Rotation effect

For the equipment we discussed in this study, the primary factor resulting in a non-uniform deposition is the rotation of the susceptor. Because they are accompanied by the rotation of the susceptor, the 4 gas inlets, which inject the reacting gases separately, lead to a non-uniform impingement of the atoms of the reacting gases on the GaN surface site. This non-uniform impingement could easily cause the irregular arrangement of the atoms on the surface site, which might provide a great deal of screw dislocations, leading to a high density of hillocks. To improve the uniformity of the atoms impinging on the surface site, a more uniform distribution of the reacting gases should be formed above the wafers. This more uniform distribution could be obtained by adjusting the flow pattern of the reacting gases. Therefore, the rotation speed has been increased to improve the uniformity of the deposition along the rotation direction. Figs. 8a and b show a comparison of the flow velocity vector distributions on the horizontal symmetry plane at 1223 K under 5 RPM and 15 RPM rotation speeds, respectively. In Fig. 8b, due to a higher rotation speed of 15 RPM, the magnitudes of the velocity vectors above the wafers are obviously more uniform than those for 5 RPM in Fig. 8a. Thus, the calculation results show that the high rotation speed will improve the uniformity of the reacting gas flow.

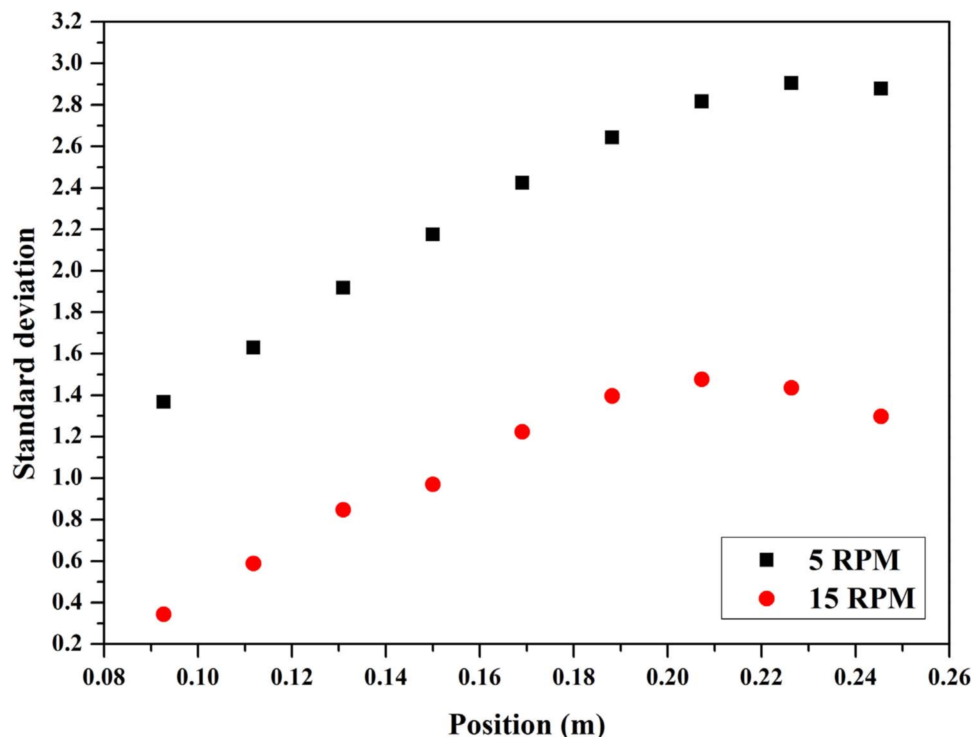

Fig. 10. Comparison of standard deviation of deposition rate along azimuthal direction between 5 RPM and 15 RPM.

The calculation results for different rotation speeds have supported the prediction that high rotation speed will improve the uniformity of the deposition rate. Figs. 8c and d show a comparison of the deposition rate distributions with different rotation speeds of 5 RPM and 15 RPM at 1223 K. Compared with the deposition rate distribution at 5 RPM in Fig. 8c, the deposition rate is larger at 15 RPM in Fig. 8d. This is because a high rotation speed of the susceptor effectively extends the residence time of the reacting gas above the susceptor, giving rise to a higher deposition rate. Moreover, the blue color (low deposition rate) has diminished in regions located between the gas inlets directions, which means that high speed rotation not only increases the deposition rate but also improves the uniformity of the deposition rate along the azimuthal direction. Fig. 9 shows the deposition rate distributions along the azimuthal direction at the rotation speed of 15 RPM. It is also observed that the deposition rate at 15 RPM is larger than that at 5 RPM (Fig. 6b). The peaks of deposition rate distribution at 15 RPM in Fig. 9 are less steep than those at 5 RPM, which means that the deposition rate fluctuation is smaller at 15 RPM. Besides, Fig. 10 shows a comparison of the standard deviations of the deposition rate along the azimuthal direction between 5 RPM and 15 RPM. The highest deviation value (1.476) in the 15 RPM case is even lower than the deviation at the center point (1.629) of P2 in the 5 RPM case. This result should demonstrate that under 15 RPM, besides the P2 and P4 wafers, the surface morphology of even P6 will be as clear as that of P2 under 5 RPM (Fig. 3). Therefore, through the calculations, it is indicated that high speed rotation will provide a more uniform gas flow pattern. The more uniform gas flow pattern results in a higher uniformity of the deposition rate along the azimuthal direction, which is a principal factor inducing hillock formation in the experiments.

4. Conclusion

In this paper, we have discussed the influence of a non-uniform deposition rate on the hillock formation in the multi-wafer horizontal HVPE equipment. Through a comparison of the hillock distributions, deposition rate along the radial direction, and deviation of the deposition rate change, it is found that the density of hillocks is related to the deposition rate fluctuations, rather than to the high deposition rate. From the calculation results of deposition rate distributions, the deposition rate change becomes small along the radial direction from center to periphery. This phenomenon is caused by the non-uniform reacting gas deposition on the surface site, which is the result of the unique system geometry with 4 separated inlets transporting the reacting gases. Therefore, to solve this problem, we have suggested that the rotation speed of the susceptor should be increased. The calculation results for a high rotation speed present a more uniform gas flow pattern and deposition rate, and a lower deviation of deposition rate change, which should prevent the formation of the hillocks at the GaN surface.

Acknowledgment

This work was supported by the National Research Foundation of Korea (NRF) grant funded by the Ministry of Science, ICT and Future Planning, Republic of Korea (MSIP) (NRF-2011-0031839).

References

[1] B. Beaumont, P. Gibart, J.P. Faurie, Nitrogen precursors in metalorganic vapor phase epitaxy of (Al,Ga)N, J. Cryst. Growth 156 (1995) 140–146.
[2] Q. Bao, M. Saito, K. Hazu, K. Furusawa, Y. Kagamitani, R. Kayano, D. Tomida, K. Qiao, T. Ishiguro, C. Yokoyama, Ammonothermal crystal growth of GaN using an NH4F mineralizer, Cryst. Growth Des. 13 (2013) 4158–4161.
[3] K. Fujito, S. Kubo, H. Nagaoka, T. Mochizuki, H. Namita, S. Nagao, Bulk GaN crystals grown by HVPE, J. Cryst. Growth 311 (2009) 3011–3014.
[4] C. Hemmingsson, G. Pozina, Optimization of low temperature GaN buffer layers for halide vapor phase epitaxy growth of bulk GaN, J. Cryst. Growth 366 (2013) 61–66.
[5] N. Liu, J. Wu, W. Li, R. Luo, Y. Tong, G. Zhang, Highly uniform growth of 2-inch GaN wafers with a multi-wafer HVPE system, J. Cryst. Growth 388 (2014) 132–136.
[6] X.-F. Han, M.-J. Hur, J.-H. Lee, Y.-j. Lee, C.-s. Oh, K.-W. Yi, Numerical simulation of the gallium nitride thin film layer grown on 6-inch wafer by commercial multi-wafer hydride vapor phase epitaxy, J. Cryst. Growth 406 (2014) 53–58.
[7] S. Hu, S. Liu, Z. Zhang, H. Yan, Z. Gan, H. Fang, A novel MOCVD reactor for growth of high-quality GaN-related LED layers, J. Cryst. Growth (2015).
[8] K. Zhou, J. Liu, S. Zhang, Z. Li, M. Feng, D. Li, L. Zhang, F. Wang, J. Zhu, H. Yang, Hillock formation and suppression on c-plane homoepitaxial GaN Layers grown by metalorganic vapor phase epitaxy, J. Cryst. Growth 371 (2013) 7–10.

[9] A. Zauner, J. Weyher, M. Plomp, V. Kirilyuk, I. Grzegory, W. Van Enckevort, J. Schermer, P. Hageman, P. Larsen, Homo-epitaxial, GaN growth on exact and misoriented single crystals: suppression of hillock formation, J. Cryst. Growth 210 (2000) 435–443.

[10] T. Wei, R. Duan, J. Wang, J. Li, Z. Huo, Y. Zeng, Hillocks and hexagonal pits in a thick film grown by HVPE, Microelectron. J. 39 (2008) 1556–1559.

[11] F. Oehler, T. Zhu, S. Rhode, M. Kappers, C. Humphreys, R. Oliver, Surface morphology of homoepitaxial < i > c < /i > -plane GaN: Hillocks and ridges, J. Cryst. Growth 383 (2013) 12–18.

[12] Y. Han, M. Caliebe, M. Kappers, F. Scholz, M. Pristovsek, C. Humphreys, Origin of faceted surface hillocks on semi-polar GaN templates grown on pre-structured sapphire, J. Cryst. Growth 415 (2015) 170–175.

[13] J.K. Kennedy, W.D. Potter, The effect of various growth parameters on the formation of pits and hillocks on the surface of epitaxial GaAs layers, J. Cryst. Growth 19 (1973) 85–89.

[14] B.J. Baliga, S.K. Ghandhi, Hillocks on epitaxial GaAs grown from trimethylgallium and arsine, J. Cryst. Growth 26 (1974) 314–316.

[15] P. Kempisty, S. Krukowski, Crystal growth of GaN on (0001) face by HVPE-atomistic scale simulation, J. Cryst. Growth 303 (2007) 37–43.

[16] C.E.C. Dam, A.P. Grzegorczyk, P.R. Hageman, R. Dorsman, C.R. Kleijn, P.K. Larsen, The effect of HVPE reactor geometry on GaN growth rate—experiments versus simulations, J. Cryst. Growth 271 (2004) 192–199.

[17] A.S. Segal, A.V. Kondratyev, S.Y. Karpov, D. Martin, V. Wagner, M. Ilegems, Surface chemistry and transport effects in GaN hydride vapor phase epitaxy, J. Cryst. Growth 270 (2004) 384–395.

[18] W. Seifert, G. Fitzl, E. Butter, Study on the growth rate in VPE of GaN, J. Cryst. Growth 52 (1981) 257–262.